JOURNAL OF VIROLOGY, May 2010, p. 4969–4978 Vol. 84, No. 10
0022-538X/10/$12.00 doi:10.1128/JVI.02623-09

Binding Site on the Transferrin Receptor for the Parvovirus Capsid and Effects of Altered Affinity on Cell Uptake and Infection▽

Laura B. Goodman,[1] Sangbom M. Lyi,[1] Natalie C. Johnson,[1] Javier O. Cifuente,[2] Susan L. Hafenstein,[2] and Colin R. Parrish[1]*

Baker Institute for Animal Health and Department of Microbiology and Immunology, College of Veterinary Medicine, Cornell University, Ithaca, New York 14853,[1] and Division of Infectious Diseases, Mail Code H036, Pennsylvania State University College of Medicine, 500 University Drive, Hershey, Pennsylvania 17033[2]

Received 15 December 2009/Accepted 23 February 2010

Canine parvovirus (CPV) and its relative feline panleukopenia virus (FPV) bind the transferrin receptor type 1 (TfR) to infect their host cells but show differences in the interactions with the feline and canine TfRs that determine viral host range and tissue tropism. We changed apical and protease-like domain residues by introducing point mutations and adding or removing glycosylation signals, and we then examined the interactions of those mutant TfRs with the capsids. Most substitutions had little effect on virus binding and uptake. However, mutations of several sites in the apical domain of the receptor either prevented binding to the capsids or reduced the affinity of receptor binding to various degrees. Glycans within the virus binding face of the apical domain also controlled capsid binding. CPV, but not the related feline parvovirus, could use receptors containing a canine TfR-specific glycosylation to mediate efficient infection, while addition of other N-linked glycosylation sites into the virus binding face of the feline apical domain reduced or eliminated both binding and infection. Replacement of critical feline TfR residue 221 with every amino acid had effects on binding and infection which were significantly associated with the biochemical properties of the residue replaced. Receptors with reduced affinities mostly showed proportional changes in their ability to mediate infection. Testing feline TfR variants for their binding and uptake patterns in cells showed that low-affinity versions bound fewer capsids and also differed in attachment to the cell surface and filopodia, but transport to the perinuclear endosome was similar.

Cell infection by animal viruses involves the attachment of the virion to one or more receptors on the plasma membrane, allowing them to enter the endosomal system or to fuse directly to the plasma membrane. Some cell receptors for viruses may act as a simple tether allowing the particle to be drawn into the cell, while others may both bind the viral protein and also induce structural changes that are necessary for infection. These specific interactions between the receptor and virus may also control the viral endosomal pathways of infection, as well as the cell and tissue tropisms and host ranges.

We are studying viruses that differ in host range. Feline panleukopenia virus (FPV) has long infected cats, whereas canine parvovirus (CPV) is a new host range variant virus that emerged in 1978 as a mutant of FPV (reviewed in reference 33). Both FPV and CPV infect cat cells by binding the feline transferrin receptor type 1 (TfR). The CPV capsid contains changes that allow it to also bind the canine TfR, and that additional binding is the critical determinant of its expanded canine host range (18, 20). The original 1978 strain of CPV, designated CPV type 2 (CPV-2), was replaced during 1979 and 1980 by a natural variant termed CPV-2a that contained five changes in the capsid protein. CPV-2 and CPV-2a capsids differ in affinity of binding to the feline TfR (21, 29), and while both are able to infect canine cells by binding the canine TfR, the affinity of attachment to that receptor is very low (29). Since 1980, additional mutants of CPV-2a have arisen (including CPV-2b and CPV-2c, due to changes of VP2 residue 426 to Asp and Glu, respectively), and those have receptor binding properties similar to those of CPV-2a. Differences in CPV capsid attachment to and uptake into canine cells compared to those with feline cells have been observed. On canine cells, the first attachment of virions occurs preferentially to filopodia rather than to receptors on the cell body, although the virus later ends up in the same endosomal compartments (17).

TfR is a type II glycoprotein that is expressed as a homodimer, and each monomer is comprised of a protease-like domain, an apical domain, and a helical domain (24). The TfRs from different species are variably glycosylated, with two N-linked glycosylations on the murine TfR, three on the human and feline TfRs (22), and four on the canine TfR (20). Transferrin (Tf) binds to TfR beneath the protease and helical domains, close to the membrane (10). The hemochromatosis protein (HFE) binds the protease-like domain and regulates Tf binding in the intestinal epithelium (7). The function of the apical domain for the normal host functions of TfR is not known.

Analysis of feline and canine TfR chimeras and mutants showed that the apical domain is involved in FPV and CPV binding, and it also controls the host-specific binding of CPV to the canine TfR (30). The specificity of binding of CPV to the canine TfR is caused by a unique Asn-linked glycosylation within the apical domain (30), and changing that conjugated Asn to Lys (as seen in the feline TfR) allows the receptor to efficiently bind FPV capsids and also greatly increases the

* Corresponding author. Mailing address: Baker Institute for Animal Health, Department of Microbiology and Immunology, College of Veterinary Medicine, Cornell University, Ithaca NY 14853. Phone: (607) 256-5649. Fax: (607) 256-5608. E-mail: crp3@cornell.edu.

▽ Published ahead of print on 3 March 2010.

binding affinity for the CPV-2 and CPV-2b capsids (30). In our previous studies we have shown that residue Leu221 in the feline TfR (equivalent to Leu212 in the human TfR) influences the binding of the receptor to both CPV and FPV capsids (30). However, the canine TfR binds the CPV capsid with an interaction distinct from that seen for the feline TfR, as many mutations in CPV prevent canine TfR binding and infection of dog cells but do not affect feline TfR binding (9, 18, 32). The differences in CPV capsids that control the specific interaction with the canine TfR alter the flexibility of capsid surface loops, suggesting that the movement of capsid surface loops is a requirement for attachment to the canine TfR and its glycans (15). When the binding of the feline TfR to CPV capsids was examined, only a small number of receptors (between one and five) bound per capsid, but the receptor attachment site on the viral surface included the positions on the 3-fold spike of the capsid that controlled canine TfR binding and canine host range (16).

The TfR is also used by other viruses for cell infection, including various New World arenaviruses and the mouse mammary tumor virus (MMTV) (34, 38, 43). The New World arenaviruses that can infect humans bind both the human and the native rodent receptors, as well as the feline TfR, while those viruses that do not infect humans do not bind the human TfR efficiently (2, 34). Binding of arenaviruses to the human TfR is determined by sequences in the receptor apical domain, including tyrosine 211 in the human TfR sequence (2, 35). Mouse mammary tumor virus glycoprotein binding to the murine TfR is influenced by sequences in the apical and protease-like domains (43).

CPV and FPV have small (25-nm) nonenveloped capsids that package a single-stranded DNA genome of ~5,120 bases. The particles are assembled from two overlapping proteins, VP1 and VP2, with ~90% of the protein being VP2. VP1 contains a 143-residue unique N-terminal sequence that encodes a phospholipase A_2 (PLA_2) enzyme (46), and that sequence also includes basic amino acid motifs that play roles in infection, likely through effects on nuclear localization (42). The VP1 unique region becomes exposed during entry without capsid disintegration, and the PLA_2 aids in endosomal escape (13, 39). For CPV most of the capsids do not leave the endosomes, and unlike Tf, they do not recycle to the cell surface (17).

Other parvoviruses bind a variety of molecules as receptors for cell infection, including glycans, such as sialic acids or heparin sulfate proteoglycans, or a variety of different glycoproteins. Some adeno-associated virus (AAV) capsids have been modified to include ligands that allow binding to alternative receptors, and those can still infect cells, suggesting that they lack structural specificity for receptor binding and cell infection (27).

Here we define structures of the feline and canine TfRs that control capsid binding and cell infection and examine the effects on those processes of changes of specific residues in the structure and of glycans within the receptor apical domain. One residue proved to have a critical role in binding, and alternative replacements at that position resulted in a variety of binding affinities and altered cell infection patterns by FPV and the different CPV strains.

MATERIALS AND METHODS

Structure modeling. The amino acid sequence of the feline TfR (NP_001009312.1) was aligned to the sequence corresponding to the crystal structure of the human TfR (1) (Protein Data Bank accession no. 3KAS) using UCSF Chimera (http://www.cgl.ucsf.edu/chimera/). Using COOT (http://www.biop.ox.ac.uk/coot/), substitutions for feline wild-type Leu at 221 were made, and the bond lengths and angles were normalized to produce a pdb file representing the predicted TfR structure with each possible amino acid substitution.

Cells, viruses, and ligands. Chinese hamster ovary (CHO)-derived cells lacking the hamster TfR (TRVb cells [26]) were grown in Ham's F-12 medium containing 5% fetal bovine serum. For virus propagation, feline NLFK cells were grown in a 1:1 mixture of McCoy's 5A and Liebovitz L15 media with 5% fetal bovine serum. Virus capsids were concentrated by polyethylene glycol precipitation followed by sucrose gradient centrifugation and then dialyzed against Dulbecco's phosphate-buffered saline (PBS) or 20 mM Tris-HCl (pH 7.5) and stored at 4°C (3, 28). For binding assays, purified capsids were conjugated to Alexa Fluor-488 (Alexa488) or Alexa594 (Invitrogen, Carlsbad, CA) (17, 20). Canine Tf (Sigma Aldrich, St. Louis, MO) was iron loaded as previously described (5, 6) and labeled with Cy5 or Texas Red.

Cloning and expression of receptor mutants. Plasmid clones of the feline or canine TfR were expressed from the pcDNA3.1(−) plasmid as previously described (31). Point mutations were introduced directly into the plasmid using the Phusion procedure (New England Biolabs, Beverly, MA) and confirmed by sequencing. The feline and canine TfRs were altered at a variety of sites predicted to be exposed on the surface of the apical and the protease-like domains, as listed in Table 1 and shown in Fig. 1A. Residue 221 in the feline TfR sequence had a critical influence on binding to both CPV and FPV capsids, and that residue was therefore mutated to all possible alternative residues to test for their effects on virus binding and cell infection. Other mutations altered residues within the apical and protease-like domains to nonconservative replacements. In some cases N-linked glycosylation sites were introduced into or removed from positions in the apical domain (Table 1).

To test binding or infection, TRVb cells were seeded into six-well trays at 2×10^4 cells per cm^2 and transfected with 2 μg of TfR plasmid using Lipofectamine according to the manufacturer's instructions (Invitrogen, Carlsbad, CA). Stable TRVb-derived cell lines expressing some of the mutant TfRs were selected by growth in the presence of 400 μg/ml of G418.

Flow cytometry. In the binding studies, cells were tested at 2 days after transfection, when they were washed twice in cold PBS and detached using Accutase (Innovative Cell Technologies, San Diego, CA). Cells were then washed in PBS with 1% ovalbumin and then incubated with 10 μg/ml of Alexa488-capsids and Cy5-Tf combined for 1 h at 37°C. The cells were finally washed in PBS-ovalbumin and fixed with 4% paraformaldehyde (PFA) in PBS. Flow cytometry was performed with a FACScalibur (BD Biosciences), analyzing at least 10,000 cells. Studies were performed in three independent replicates.

For assaying infection by flow cytometry, TRVb cells were seeded and transfected as described above, incubated for 2 days, washed with Dulbecco's modified Eagle's medium (DMEM) with 0.1% bovine serum albumin (BSA), inoculated with viruses, and incubated for 2 days at 37°C. The cells were then detached as described above and first incubated with Cy5-labeled Tf for 1 h. The cells were then fixed and permeabilized using an intracellular staining preparation kit (eBioscience, San Diego, CA) and stained for viral proteins using a polyclonal anti-CPV rabbit serum labeled with fluorescein isothiocyanate (FITC). Cells were finally resuspended in PBS with 1% ovalbumin and 0.09% sodium azide and analyzed by flow cytometry as described above.

Fluorescence microscopy. Stable TRVb cell lines expressing variant TfRs were seeded at a density of 1×10^4 cells/cm^2 in coverslip dishes (MatTek, Ashland, MA) and then used for experiments 2 days later. To detect the early stages of entry, the TfR cell lines were incubated with Alexa488– or Alexa594–CPV-2 capsids or with Texas Red- or Alexa488-labeled Tf at 37°C in phenol-red free DMEM. The binding and distribution of the virus or Tf were observed within 15 min of incubation, and then the cells were washed and incubated at 37°C for various times (17). Cells were also fixed with 4% paraformaldehyde after 15, 30, or 60 min of incubation at 37°C. Images were collected with a Hamamatsu OrcaER camera, with different labels collected as separate channels, and then analyzed using the SimplePCI software (Hamamatsu, Sewickley, PA).

Statistical analyses. Flow cytometry data were analyzed using FlowJo v.9 (TreeStar, Ashland, OR). After gating based on cell size/granularity, differences between the raw fluorescence data of the samples were statistically tested using the multivariate probability binning method (36, 37). In a second analysis, we gated the cells based on staining patterns, exported the raw fluorescence data for cells positive for both CPV and Tf, and further analyzed using statistical software

TABLE 1. Feline TfR mutants prepared in these studies[a]

Domain	Feline TfR mutation[b]	Human TfR position
Wild-type feline	—	—
Apical, deletion	ΔV201-V390[c]	ΔV192-V380
Apical, feline to canine changes (canine unique glycosylation site introduced)	G203S/N205ins/S207Q/K383N/S385T	D194/196/Q198/K374/T376
Apical (glycosylation site introduced)	V212N	203
Apical (altered to all other residues)	L221X (L221C[c])	L212
Apical (glycosylation site removed)	N326Y[c]	N317
	N260R	N251
Apical	N284K	N275
	N254K	D245
	T300D	V291
	T214A	K205
	D369K	D360
	N256F	Y247
	R378D[c]	E369
Protease-like	E583K	K574
	Q587K	E578
	K588D	R579
	D569K	D560
	D534K	D525
	I538D	A529

[a] Controls included the wild-type canine TfR and the canine TfR with the unique glycosylation site (N383/T385) removed (30).
[b] —, no mutation (wild type); Δ, deletion between the indicated residues in the feline TfR.
[c] Receptor did not reach the cell surface (indicated with the notation "NCS" in Fig. 3 to 5).

JMP 8 (SAS, Cary, NC). The CPV/Tf dual-positive data for each of the three replicates of the TfR clones tested were fitted to regression curves and transformed by multiplying the inverse by 10. Samples which had no intercept were either assigned an intercept of zero (those which bound Tf but not virus) or marked "NCS" (no cell surface expression) (for those which did not bind Tf or virus because they did not reach the cell surface). Stable cell lines of TRVb cells expressing the TfR variants were also tested for Tf binding levels using fluorescence microscopy, where cells were incubated with labeled Tf and photographed under equivalent conditions, and the digital images were compared using NIH ImageJ (http://rsbweb.nih.gov/ij/).

RESULTS

Receptor mutants affecting capsid binding are highly focused. In order to define the specific binding features of the TfR and the effects of altered receptors on cell infection by parvoviruses, we prepared a number of mutants of the feline TfR with altered surface residues in the apical and protease-like domains (Table 1; Fig. 1A). All mutant TfRs were expressed in receptor-negative TRVb cells, screened for binding and uptake of labeled capsids and canine Tf at 37°C, and compared to the wild-type TfR in parallel (the method is illustrated in Fig. 2). Several statistical methods were used to compare the results for the mutant TfRs to those for the wild-type feline TfR, including a robust chi-square-based analysis designed for flow cytometry (36, 37). This test was utilized to compare the overall differences in virus and Tf binding or infection. Due to normal variation in receptor expression levels caused by transfection efficiency, cell dissociation efficacy, and other possible factors, some variant receptors appeared to have lower percentages of virus/Tf dual-positive cells, but virus binding was actually statistically similar to that for the wild type. We therefore did a secondary analysis of the intercept of the virus-Tf regression. Since the binding site of human Tf is distant from the mutations we made (Fig. 1) (10), we did not expect most of the mutants to affect Tf binding, and this was seen in the study. Some variant receptors, including one of the glycosylation mutants, did not traffic to the cell surface, and those therefore did not show either Tf or virus attachment (indicated as "not cell surface" [NCS] in the figures).

Changes of most positions within the apical and protease-like domains of the receptors had little effect on virus binding or CPV infection, although the replacements of Thr300 with Asp and of Asp369 with Lys reduced both binding and infection (Table 1; Fig. 1 and 3). The most striking effects were seen for replacements of Leu221 in the feline TfR sequence (equivalent to residue 212 of the human TfR), which showed reduced virus binding (Table 1; Fig. 1, 2, and 4). When that codon was changed to express each of the other possible residues, a range of effects on virus attachment was seen, varying from no detectable binding up to binding that was equal to that of the wild-type receptor (Fig. 2 and 4). Specific virus binding levels were determined by comparing the virus and Tf levels on the same cells using flow cytometry (Fig. 2 to 5). We have shown previously that Tf binding to the feline TfR does not influence virus binding (30), and that was confirmed here (results not shown), and the capsid binding efficiencies were therefore determined from the ratios of the virus and Tf binding levels. The lower-binding TfR mutants allowed virus binding only when cells expressed the highest levels of TfR, where they bound as much as 100-fold more TfR than the wild type to give the same level of virus binding. Virus binding avidities were then compared by taking the *y* axis intercept of cells that showed virus binding, and the reciprocals of the data are shown in the figures to allow the direct comparison with data from infection assays (Fig. 3 to 5A). TfR mutants showing no detectable capsid binding were reported as 0, as there was no intercept.

To understand the effects of the replacements on the struc-

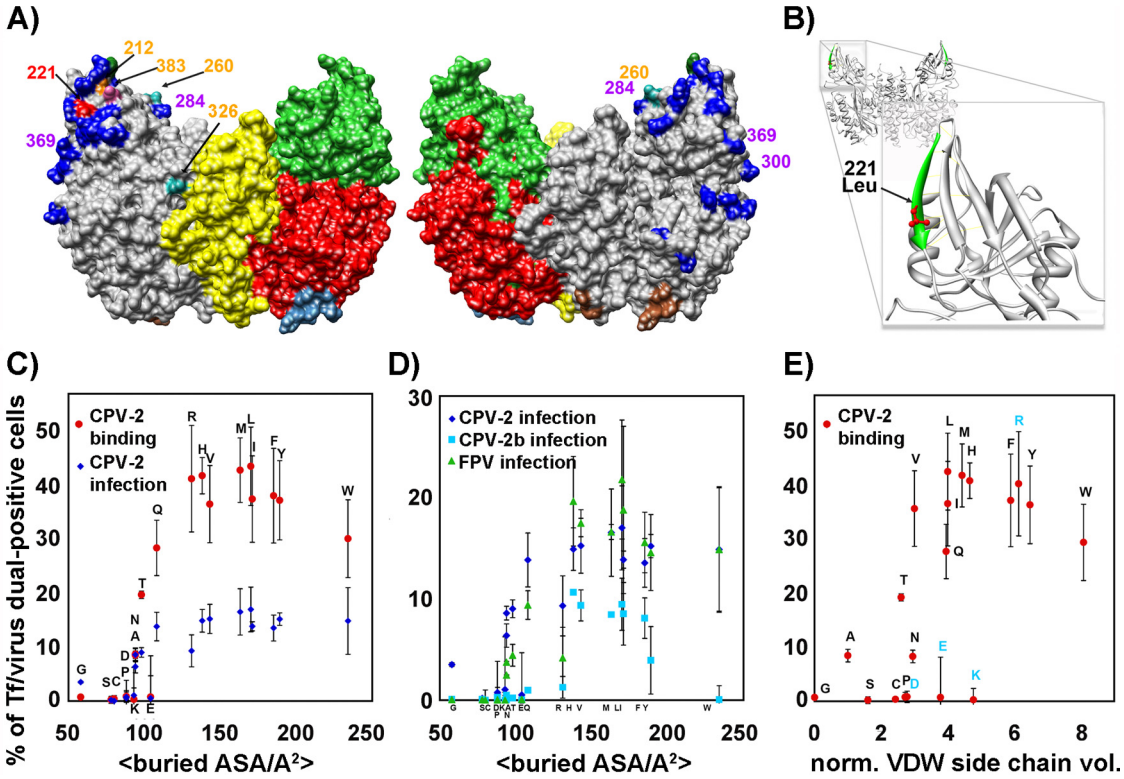

FIG. 1. (A) Locations of mutations tested, shown on a model of the feline sequence aligned to the human TfR structure. The different domains are colored in green (apical), red (protease-like), and yellow (helical). A portion of the stalk domain is colored in cyan (left), and the sites associated with Tf binding are brown (right). The following color code is used on the gray portion of the structure to highlight the substitutions which were made: red, Leu221; cyan, conserved N-linked glycosylation sites; orange, new glycosylation site added; pink, canine TfR unique glycosylation site added; dark blue, all other sites mutated in these studies. Changes with a large effect on virus binding are indicated by labels in red or purple. The labels of all the Asn-linked glycosylation sites are orange. (B) The position of residue Leu221 within the apical domain, shown in a model derived from the human TfR (the human position is Leu212). (C) Binding of CPV-2 capsids or infection by CPV-2 virus (as the percentage of positive cells) when using feline TfRs containing the indicated changes of residue 221, compared to the average buried accessible surface area (ASA) of the amino acid expressed. (D) Infection by CPV-2, CPV-2b, or FPV (shown as the percentage infection-positive cells) of cells expressing feline TfRs containing the indicated changes of residue 221, compared to average buried ASA of the amino acid expressed. (E) Binding of CPV-2 capsids to cells expressing feline TfRs containing the indicated changes of residue 221, compared to normalized van der Waals (VDW) side chain volumes of the replacement residues. Error bars indicate standard deviations.

ture and virus binding, we examined their effects on a model derived from the human TfR structure that has been refined in a recent study by Abraham et al. (1). That model revealed that residue 221 is within a β-strand which is part of a β-sheet that is likely conserved between human and feline TfRs. There were no predicted intramolecular interactions with the side chain of the conserved feline Leu221, which is surface exposed and extending away from the neighboring β-strand (Fig. 1B).

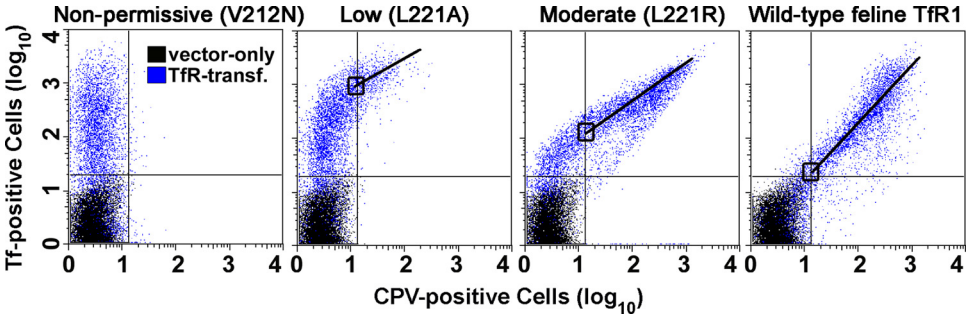

FIG. 2. Methods used for analyzing virus binding by the variant forms of the TfR. Representative examples of different binding profiles are shown, with Tf and virus (CPV-2) binding assayed by flow cytometry in transfected TRVb cells. The lines superimposed on the graphs represent regressions of the data in the upper right quadrant, and the intercept of the regression line with the axis between the Tf-positive and dual-stained quadrants shows the level of TfR expression (measured as Tf binding) required for detectable virus binding. Each panel represents three independent replicates of at least 10,000 cells, which were concatenated to make these plots.

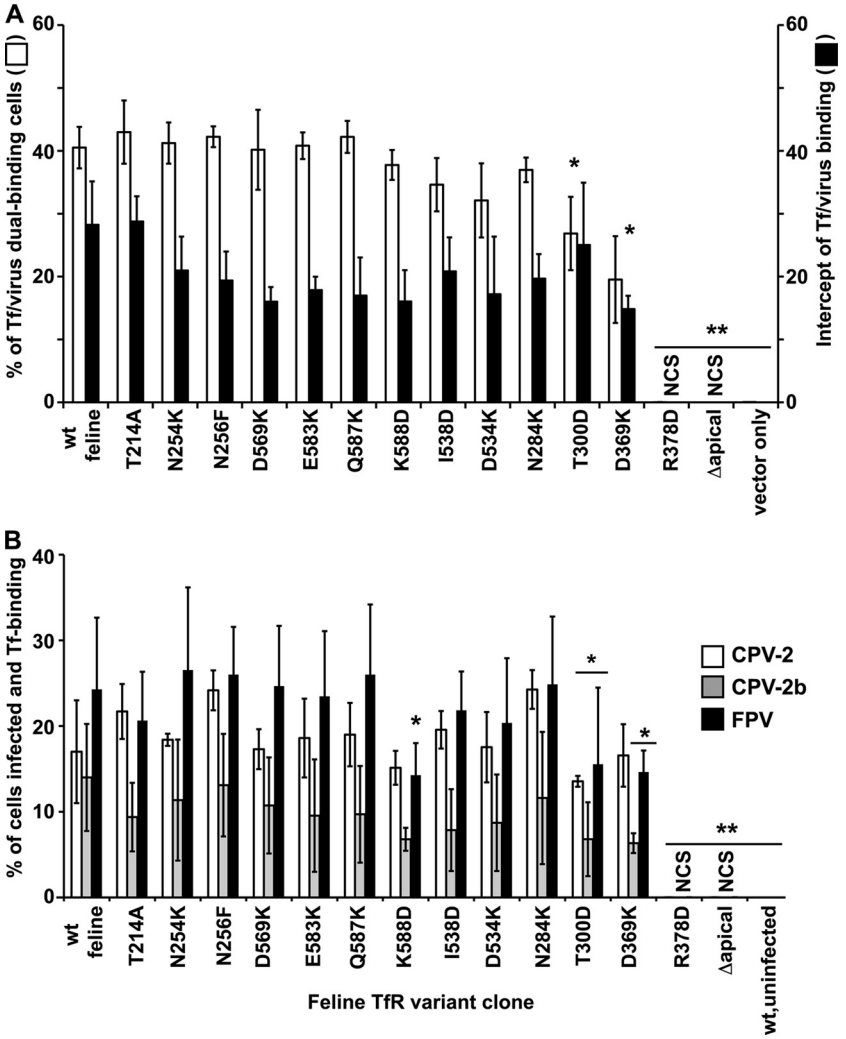

FIG. 3. Effects of replacements of various residues in the apical and protease-like domains of the feline TfR on the binding of virus and on virus infection, compared to those with the wild-type (wt) feline TfR. Means and standard deviations from three independent experiments are shown. Receptors not reaching the cell surface are indicated with the notation "NCS." Statistically significant differences from the results seen for the wild-type feline TfR are noted (*, $P < 0.05$; **, $P < 0.01$); these were determined by testing the raw fluorescence data (not the mean values of percent bound or infected cells shown). (A) As illustrated in Fig. 2, flow cytometry was used to determine CPV-2 binding. Results of both analyses of viral binding are shown (percent dual CPV-2/Tf positive and intercept between the *y* axis of the Tf binding versus CPV-2 binding). The intercept represents the level of TfR expression on cells required to allow detectable virus attachment and uptake (here presented as the inverse for visual comparison) with cells not binding virus assigned an intercept of zero. (B) Infection of transfected TRVb cells with CPV-2, CPV-2b, and FPV. Cells were assayed by antibody staining combined with labeled Tf uptake and flow cytometry.

We examined the relationships between known amino acid parameters of the replacements of residue 221 and our experimental observations on binding and infection. We examined the correlation between the character of the side chain and binding effects of the mutant receptor. Properties examined included charge, polarity, normalized van der Waals (VDW) volume, hydrophobicity and localized electrical effect (14); hydropathy index (23); electronic charge and isotropic surface area (11); and accessible surface area (ASA), average buried ASA, and burial propensity (47). The average buried ASA (47) was the only parameter that displayed a direct correlation ($P < 0.001$) to the alterations in binding and infection, followed by a close correlation with VDW side chain volume ($P = 0.004$) and binding.

Buried ASA measurements have been used previously to describe the effects of mutations on the interactions between macromolecules (4, 12). Here, average buried ASA values (47) describe the surface buried away from solvent when virus and TfR associate to form a complex, and they likely have a direct relationship with complex stability. Residue 221 could be defined as a "hot spot," such as other authors have shown for antibody-protein complexes (40), with mutational analyses and structural evidence suggesting that residue 221 would be buried in the receptor-virus interface. Our analysis indicates that there is a range of buried ASA values which are favorable to the interactions and contribute to complex stability (high virus binding), while residues outside that range cause the complex to lose stability and show low virus binding. Average buried

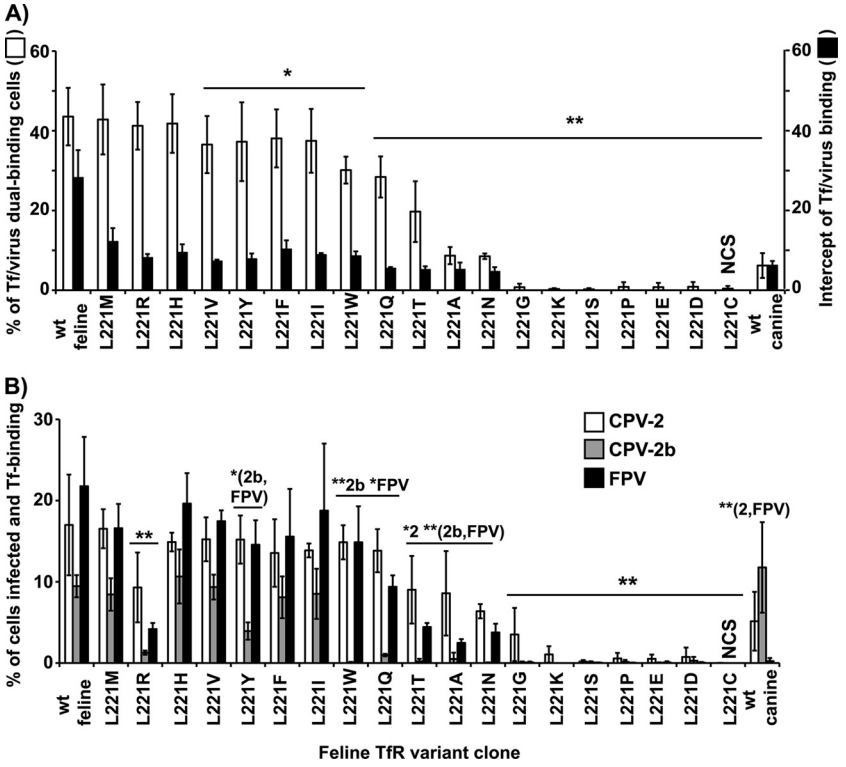

FIG. 4. Effects of all replacements of residue 221 of the feline TfR on virus binding and virus infection. Virus binding (A) and infection (B) are shown as described in the legend of Fig. 3.

ASA values of between 130 and 190 Å^2 corresponded to high binding, while outside this range the binding dropped (Fig. 1C). For each substitution except Arg, the effect on infectivity corresponded to the effect on binding (Fig. 1C and D and 4). Arginine has an average buried ASA of 131 Å^2, which is within the preferred range for binding, but shows a significant decrease in infectivity, suggesting that the charge of the Arg side chain causes a reduction in infectivity. The correlation between binding/infection and van der Waals side chain volume is slightly different, being more affected by the charge of the residue side chain (Fig. 1E), suggesting that van der Waals forces also govern the interaction between virus and TfR at residue 221 (12).

Altering glycosylation sites. The specificity of the canine TfR for CPV capsids is largely due to the unique N-linked glycan attached to Asn383 (feline TfR numbering), and the viral sequences that control binding to the canine TfR include VP2 residues 93, 299 or 300, and 323 (21). To further examine the role of glycosylation in the control of virus binding, we replaced residue 212 with an Asn, to give a new glycosylation site, and also changed the glycosylated Asn residues 260 and 326 (Fig. 5). The feline TfR with Asn212 showed normal levels of Tf binding but greatly reduced virus binding (Fig. 5). The canine TfR with the unique glycosylation site mutated to Lys (as in the feline TfR sequence) showed increased capsid binding (30). Altering residue Asn326 prevented receptor transport to the cell surface, while modification of glycosylation site Asn260 within the apical domain allowed cell surface receptor expression and resulted in only a small reduction in virus binding and a CPV-2b strain-specific reduction in infection (Fig. 5).

Effects on virus infection of cells. In most cases there was a close correlation between the level of binding of the mutant TfRs to the virus and the efficiency of cell infection. Those receptors that showed no or low virus binding allowed no or little infection, while those that showed intermediate effects on binding allowed intermediate infection compared to the wild-type receptor (Fig. 2 to 5). For the low-binding receptors, the cells that became infected were those that showed the highest levels of TfR expression (as detected by Tf binding levels), while for the wild-type feline TfR, cells were infected when they expressed 10-fold less receptor or even lower levels (Fig. 2).

Virus strain-specific binding and infection. The natural virus strains FPV, CPV-2, and CPV-2b differ in binding affinity and specificity for the feline and canine TfRs, and we therefore compared their binding and cell infection using the mutant TfRs. There were differences in the number of receptors required to allow infection by the different virus strains (Fig. 3 to 5B), indicating strain-specific differences in the control of infection. Specifically, CPV-2 showed similar levels of infection, while CPV-2b and FPV strains showed lower levels of infection for several of the mutant TfRs. This indicates a different interaction of some virus strains with the feline TfR, which may be modulating later stages in the infection process.

Effects of mutants on binding to and uptake into cells. We recently reported that the initial binding of CPV capsids to canine and feline cells differs in the attachment to filopodia or

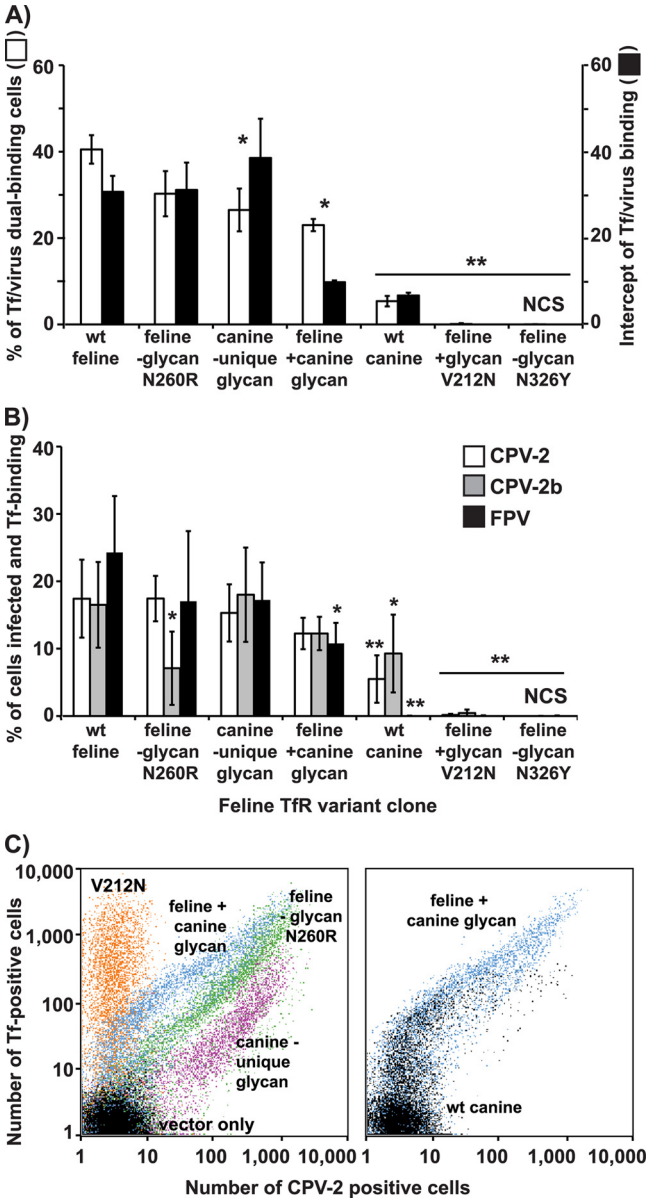

FIG. 5. Characterization of feline and canine TfR mutants with alterations in glycosylation patterns, including either addition (V212N and K383N/S385T) or removal (N260R and N326Y) of sites within the apical domain, or the canine TfR with the unique glycosylation site (N383/T385) removed (30). Virus binding (A) and infection (B) are shown as described in the legend of Fig. 3, and representative binding profiles are compared (C).

to the cell body (17), and this was suggested to be due to differences in the affinity of the interaction with the canine and feline TfRs. Here we examined this difference directly by examining the attachment and uptake patterns of viruses by a feline TfR with a single change that resulted in lower virus binding, Leu221Ala (Fig. 2 and 6). Tf binding was similar for both receptors (Fig. 2 and 6A). While capsid binding to receptors on the cell body was seen on cells expressing the wild-type feline TfR, the Leu221Ala mutant showed more capsid binding to the filopodia (Fig. 6B); at later times of incubation, capsids accumulated inside the cell (Fig. 6B).

DISCUSSION

Here we have identified and characterized specific sites on the TfR that directly control binding to CPV and related viruses. The interaction of the feline TfR with CPV-2 capsids was affected by replacements in residue 221 in one face of the apical domain, as well as residues 300 and 369 on the "end" of that domain. Other residues in the apical domain had no effect, and neither did the changes tested in the protease-like domains. Similar levels of infection were seen for the three viral strains tested, but CPV-2b and FPV had lower rates for some TfR variants. A critical and amino acid-dependent virus interaction with the TfR is controlled by residue 221 (Fig. 4), a conserved residue that is exposed on the human TfR surface and on models of the feline TfR (Fig. 1). Modifications in N-linked glycosylation sites also had significant effects, including complete inhibition of binding and infection (Fig. 5).

We prepared a series of receptors altered in only residue 221 that showed various levels of virus binding, ranging from not detectable to equal to the wild-type level. The direct correlation of virus binding and infection with buried ASA and VDW volume suggests that the 221 site is within the TfR structure that allows virus recognition and the formation of stable virus-receptor interactions. The residues with the smallest average buried surface areas and volumes may not allow an interaction with the virus, due to the insufficient volume or altered topology of the binding site. Since a Trp at position 221 also caused reduced binding and infection, it appears that too large a volume also causes surface changes that hinder the interaction with virus. Thus, the actual topology of the TfR at the site of residue 221 is critical, identifying a "hot spot," a unique residue within the broad footprint of TfR on the virus surface that controls binding and infection.

Some viral receptors appear to make critical structural interactions with the viral protein that are required for infection, while others appear to act as simple tethers and not to play a structural role. For CPV and FPV a structural role has been suggested, due the observation that sialic acids can bind CPV or FPV to the surface of cells but do not mediate infection, and neither do receptors prepared with binding domains derived from antiviral antibodies (19, 41). This question is not completely resolved here. Most of the mutations of residues that reduce capsid binding cause a proportional reduction in virus infection, except in the case of Arg221, which has a greater effect on infection than binding, suggesting that some specific interactions between virus and receptor may affect later steps in the infectious process.

That relationship between affinity and infectivity was not seen for the canine TfR, which had a low affinity of CPV-2 binding, similar to that seen for the Ala or Asn mutations of residue 221 in the feline TfR. That receptor allowed approximately 2-fold-higher levels of infection by CPV-2b than by CPV-2 and allowed no infection by FPV. This likely resulted from the adaptive process of the CPV in dogs, which allowed the efficient use of the canine TfR in nature in newer strains.

The sequence of the TfR apical domain is quite conserved, but its natural function for the host is still unknown, and it does not interact with known TfR ligands, including Tf or HFE (7). When the entire apical domain was deleted, the receptor was not transported to the cell surface (Fig. 3). The apical domain

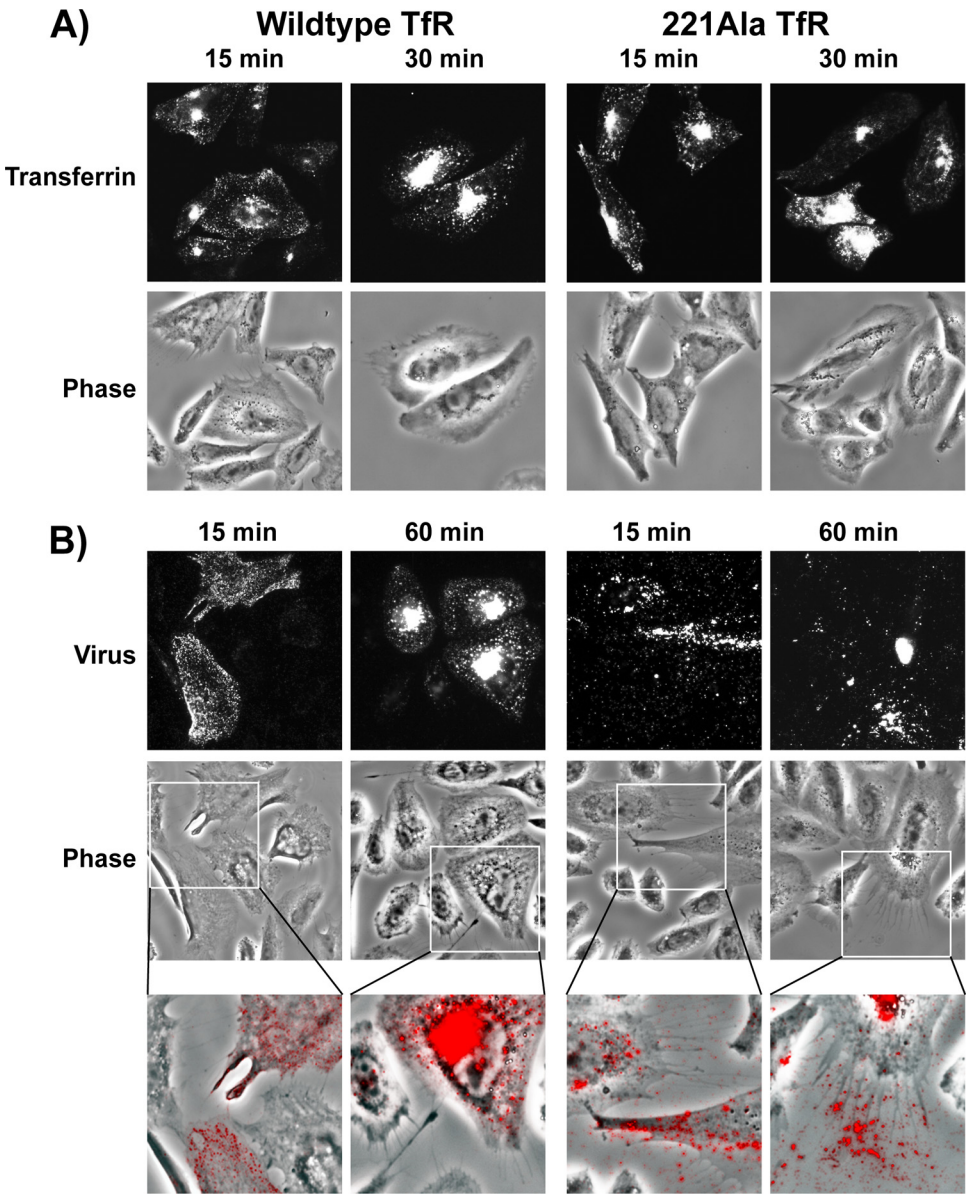

FIG. 6. Binding and uptake patterns of Tf or virus on TRVb cells expressing the wild-type feline TfR or the Ala221 mutant feline TfR, that shows a low affinity of virus attachment. (A) Cells after incubation with Tf for 15 or 30 min at 37°C, as indicated, and fixation with paraformaldehyde. A light microscopy image (phase) is shown, as well as a fluorescence image of labeled Tf (transferrin). (B) Cells after incubation with Alexa594-virus for 15 or 60 min at 37°C, as indicated, and fixation with paraformaldehyde. A light microscopy image (phase) is shown, as well as a fluorescence image of labeled capsids (virus). A magnified view shows an overlay of the cell phase image with the labeled capsids, with the association of virus with the filopodia on cells expressing the Ala221 TfR but not the wild type.

structure appears to be a "viral binding patch," as the same TfR structure is also targeted by other pathogens, including the New World arenaviruses and MMTV (35, 43). Binding to murine or human TfRs by the New World arenaviruses is controlled by a residue (211 in the human TfR) that is immediately adjacent to the human Leu212 (feline TfR residue 221) that controls binding of these parvovirus capsids (2). In the case of the arenavirus binding to the TfR, the feline but not the canine TfR also binds the glycoproteins of four different arenaviruses (2). That host specificity is also controlled by sequences in the apical domain, perhaps in part by the additional glycan on the canine TfR. Such a receptor structure that is bound by multiple viruses has been suggested for angiotensin-converting hormone receptor 2, which has a small region that is bound by at least two different coronaviruses (44). The reasons for these sites on receptors that bind multiple viruses are not known, but they may involve some feature of their structure or other consequences of the virus-host coevolution.

Receptor glycosylation controls virus binding. The canine TfR specificity for CPV is controlled primarily by a single additional glycosylation site within the apical domain, and CPV gained the ability to bind the canine TfR without losing its ability to bind the feline TfR. Here we also showed reduced binding to the feline TfR by adding a novel glycosylation site at

feline TfR position 212. CPV binding to the canine TfR is associated with the flexibility of surface loops that likely allow the capsid surface to accommodate the added glycan in the apical domain of the canine TfR (15, 25, 28), but those changes did not allow it to accommodate the novel glycan. Some glycosylations of the human TfR, such as that attached to residue 317, are required for correct folding and transport to the plasma membrane (8, 45). Changing the equivalent position in the feline TfR (Asn326Tyr) prevented the receptor from reaching the cell surface (Fig. 5). Changing the other highly conserved site at feline TfR residue 260 reduced levels of infection by CPV-2b but not by CPV-2 or FPV.

TfR affinity and patterns of entry. In previous studies we observed virus binding to feline cells over the cell surface but attachment to canine cells that was initially to filopodia, and that was hypothesized to be due to differences in the affinities of binding to the feline and canine TfRs (17). Here we observed that the low-affinity Leu221Ala variant of the feline TfR gave specific capsid binding to filopodia when it was expressed on TRVb cells and that capsid (but not Tf) binding was at a much lower level than was seen for the wild-type feline TfR. However, after attachment the bound virus was able to enter the endosomal system, as seen for dog and cat cells (17).

These studies confirm the specific nature of the interactions between the TfR and the CPV and FPV capsids and identify a particular role for the interaction of the receptor apical domain and the capsid. In future studies we wish to identify the residues in the capsids that control the binding to affinity-altered receptors.

ACKNOWLEDGMENTS

This work was supported by the following grants from the National Institutes of Health: AI28385 and AI33468 to C.R.P., AI079271 to S.L.H., and AI082922 to L.B.G.

Stephen C. Harrison provided the crystal structure of the human TfR1. Wendy S. Weichert and Virginia Scarpino provided excellent technical support. The Cornell Statistical Consulting Unit and TreeStar, Inc., provided analytical support.

REFERENCES

1. **Abraham, J., K. D. Corbett, M. Farzan, H. Choe, and S. C. Harrison.** 7 March 2010, posting date. Structural basis for receptor recognition by New World hemorrhagic fever arenaviruses. Nat. Struct. Mol. Biol. doi:10.1038/nsmb.1772.
2. **Abraham, J., J. A. Kwong, C. G. Albarino, J. G. Lu, S. R. Radoshitzky, J. Salazar-Bravo, M. Farzan, C. F. Spiropoulou, and H. Choe.** 2009. Host-species transferrin receptor 1 orthologs are cellular receptors for nonpathogenic New World clade B arenaviruses. PLoS Pathog. **5:**e1000358.
3. **Agbandje, M., R. McKenna, M. G. Rossmann, M. L. Strassheim, and C. R. Parrish.** 1993. Structure determination of feline panleukopenia virus empty particles. Proteins **16:**155–171.
4. **Arnold, E., and M. G. Rossmann.** 1990. Analysis of the structure of a common cold virus, human rhinovirus 14, refined at a resolution of 3.0 Å. J. Mol. Biol. **211:**763–801.
5. **Bates, G. W., and M. R. Schlabach.** 1973. The reaction of ferric salts with transferrin. J. Biol. Chem. **248:**3228–3232.
6. **Bates, G. W., and J. Wernicke.** 1971. The kinetics and mechanism of iron(3) exchange between chelates and transferrin. IV. The reaction of transferrin with iron(3) nitrilotriacetate. J. Biol. Chem. **246:**3679–3685.
7. **Bennett, M. J., J. A. Lebron, and P. J. Bjorkman.** 2000. Crystal structure of the hereditary haemochromatosis protein HFE complexed with transferrin receptor. Nature **403:**46–53.
8. **Byrne, S. L., R. Leverence, J. S. Klein, A. M. Giannetti, V. C. Smith, R. T. MacGillivray, I. A. Kaltashov, and A. B. Mason.** 2006. Effect of glycosylation on the function of a soluble, recombinant form of the transferrin receptor. Biochemistry **45:**6663–6673.
9. **Chang, S. F., J. Y. Sgro, and C. R. Parrish.** 1992. Multiple amino acids in the capsid structure of canine parvovirus coordinately determine the canine host range and specific antigenic and hemagglutination properties. J. Virol. **66:**6858–6867.
10. **Cheng, Y., O. Zak, P. Aisen, S. C. Harrison, and T. Walz.** 2004. Structure of the human transferrin receptor-transferrin complex. Cell **116:**565–576.
11. **Collantes, E. R., and W. J. Dunn III.** 1995. Amino acid side chain descriptors for quantitative structure-activity relationship studies of peptide analogues. J. Med. Chem. **38:**2705–2713.
12. **Ding, J., A. Jacobo-Molina, C. Tantillo, X. Lu, R. G. Nanni, and E. Arnold.** 1994. Buried surface analysis of HIV-1 reverse transcriptase p66/p51 heterodimer and its interaction with dsDNA template/primer. J. Mol. Recognit. **7:**157–161.
13. **Farr, G. A., L. G. Zhang, and P. Tattersall.** 2005. Parvoviral virions deploy a capsid-tethered lipolytic enzyme to breach the endosomal membrane during cell entry. Proc. Natl. Acad. Sci. U. S. A. **102:**17148–17153.
14. **Fauchere, J. L., M. Charton, L. B. Kier, A. Verloop, and V. Pliska.** 1988. Amino acid side chain parameters for correlation studies in biology and pharmacology. Int. J. Pept. Protein Res. **32:**269–278.
15. **Govindasamy, L., K. Hueffer, C. R. Parrish, and M. Agbandje-McKenna.** 2003. Structures of host range-controlling regions of the capsids of canine and feline parvoviruses and mutants. J. Virol. **77:**12211–12221.
16. **Hafenstein, S., L. M. Palermo, V. A. Kostyuchenko, C. Xiao, M. C. Morais, C. D. Nelson, V. D. Bowman, A. J. Battisti, P. R. Chipman, C. R. Parrish, and M. G. Rossmann.** 2007. Asymmetric binding of transferrin receptor to parvovirus capsids. Proc. Natl. Acad. Sci. U. S. A. **104:**6585–6589.
17. **Harbison, C. E., S. M. Lyi, W. S. Weichert, and C. R. Parrish.** 2009. Early steps in cell infection by parvoviruses: host-specific differences in cell receptor binding but similar endosomal trafficking. J. Virol. **83:**10504–10514.
18. **Hueffer, K., L. Govindasamy, M. Agbandje-McKenna, and C. R. Parrish.** 2003. Combinations of two capsid regions controlling canine host range determine canine transferrin receptor binding by canine and feline parvoviruses. J. Virol. **77:**10099–10105.
19. **Hueffer, K., L. M. Palermo, and C. R. Parrish.** 2004. Parvovirus infection of cells by using variants of the feline transferrin receptor altering clathrin-mediated endocytosis, membrane domain localization, and capsid-binding domains. J. Virol. **78:**5601–5611.
20. **Hueffer, K., J. S. Parker, W. S. Weichert, R. E. Geisel, J. Y. Sgro, and C. R. Parrish.** 2003. The natural host range shift and subsequent evolution of canine parvovirus resulted from virus-specific binding to the canine transferrin receptor. J. Virol. **77:**1718–1726.
21. **Hueffer, K., and C. R. Parrish.** 2003. Parvovirus host range, cell tropism and evolution. Curr. Opin. Microbiol. **6:**392–398.
22. **Hunt, R. C., R. Riegler, and A. A. Davis.** 1989. Changes in glycosylation alter the affinity of the human transferrin receptor for its ligand. J. Biol. Chem. **264:**9643–9648.
23. **Kyte, J., and R. F. Doolittle.** 1982. A simple method for displaying the hydropathic character of a protein. J. Mol. Biol. **157:**105–132.
24. **Lawrence, C. M., S. Ray, M. Babyonyshev, R. Galluser, D. W. Borhani, and S. C. Harrison.** 1999. Crystal structure of the ectodomain of human transferrin receptor. Science **286:**779–782.
25. **Llamas-Saiz, A. L., M. Agbandje-McKenna, J. S. L. Parker, A. T. M. Wahid, C. R. Parrish, and M. G. Rossmann.** 1996. Structural analysis of a mutation in canine parvovirus which controls antigenicity and host range. Virology **225:**65–71.
26. **McGraw, T. E., L. Greenfield, and F. R. Maxfield.** 1987. Functional expression of the human transferrin receptor cDNA in Chinese hamster ovary cells deficient in endogenous transferrin receptor. J. Cell Biol. **105:**207–214.
27. **Michelfelder, S., and M. Trepel.** 2009. Adeno-associated viral vectors and their redirection to cell-type specific receptors. Adv. Genet. **67:**29–60.
28. **Nelson, C. D., E. Minkkinen, M. Bergkvist, K. Hoelzer, M. Fisher, B. Bothner, and C. R. Parrish.** 2008. Detecting small changes and additional peptides in the canine parvovirus capsid structure. J. Virol. **82:**10397–10407.
29. **Palermo, L. M., S. L. Hafenstein, and C. R. Parrish.** 2006. Purified feline and canine transferrin receptors reveal complex interactions with the capsids of canine and feline parvoviruses that correspond to their host ranges. J. Virol. **80:**8482–8492.
30. **Palermo, L. M., K. Hueffer, and C. R. Parrish.** 2003. Residues in the apical domain of the feline and canine transferrin receptors control host-specific binding and cell infection of canine and feline parvoviruses. J. Virol. **77:**8915–8923.
31. **Parker, J. S., W. J. Murphy, D. Wang, S. J. O'Brien, and C. R. Parrish.** 2001. Canine and feline parvoviruses can use human or feline transferrin receptors to bind, enter, and infect cells. J. Virol. **75**:3896–3902.
32. **Parker, J. S., and C. R. Parrish.** 1997. Canine parvovirus host range is determined by the specific conformation of an additional region of the capsid. J. Virol. **71:**9214–9222.
33. **Parrish, C. R., and Y. Kawaoka.** 2005. The origins of new pandemic viruses: the acquisition of new host ranges by canine parvovirus and influenza A viruses. Annu. Rev. Microbiol. **59:**553–586.
34. **Radoshitzky, S. R., J. Abraham, C. F. Spiropoulou, J. H. Kuhn, D. Nguyen, W. Li, J. Nagel, P. J. Schmidt, J. H. Nunberg, N. C. Andrews, M. Farzan, and H. Choe.** 2007. Transferrin receptor 1 is a cellular receptor for New World haemorrhagic fever arenaviruses. Nature **446:**92–96.

35. **Radoshitzky, S. R., J. H. Kuhn, C. F. Spiropoulou, C. G. Albarino, D. P. Nguyen, J. Salazar-Bravo, T. Dorfman, A. S. Lee, E. Wang, S. R. Ross, H. Choe, and M. Farzan.** 2008. Receptor determinants of zoonotic transmission of New World hemorrhagic fever arenaviruses. Proc. Natl. Acad. Sci. U. S. A. **105:**2664–2669.
36. **Roederer, M., W. Moore, A. Treister, R. R. Hardy, and L. A. Herzenberg.** 2001. Probability binning comparison: a metric for quantitating multivariate distribution differences. Cytometry **45:**47–55.
37. **Roederer, M., A. Treister, W. Moore, and L. A. Herzenberg.** 2001. Probability binning comparison: a metric for quantitating univariate distribution differences. Cytometry **45:**37–46.
38. **Ross, S. R., J. J. Schofield, C. J. Farr, and M. Bucan.** 2002. Mouse transferrin receptor 1 is the cell entry receptor for mouse mammary tumor virus. Proc. Natl. Acad. Sci. U. S. A. **99:**12386–12390.
39. **Suikkanen, S., M. Antila, A. Jaatinen, M. Vihinen-Ranta, and M. Vuento.** 2003. Release of canine parvovirus from endocytic vesicles. Virology **316:** 267–280.
40. **Sundberg, E. J., M. Urrutia, B. C. Braden, J. Isern, D. Tsuchiya, B. A. Fields, E. L. Malchiodi, J. Tormo, F. P. Schwarz, and R. A. Mariuzza.** 2000. Estimation of the hydrophobic effect in an antigen-antibody protein-protein interface. Biochemistry **39:**15375–15387.
41. **Tresnan, D. B., L. Southard, W. Weichert, J. Y. Sgro, and C. R. Parrish.** 1995. Analysis of the cell and erythrocyte binding activities of the dimple and canyon regions of the canine parvovirus capsid. Virology **211:**123–132.
42. **Vihinen-Ranta, M., D. Wang, W. S. Weichert, and C. R. Parrish.** 2002. The VP1 N-terminal sequence of canine parvovirus affects nuclear transport of capsids and efficient cell infection. J. Virol. **76:**1884–1891.
43. **Wang, E., L. Albritton, and S. R. Ross.** 2006. Identification of the segments of the mouse transferrin receptor 1 required for mouse mammary tumor virus infection. J. Biol. Chem. **281:**10243–10249.
44. **Wu, K., W. Li, G. Peng, and F. Li.** 2009. Crystal structure of NL63 respiratory coronavirus receptor-binding domain complexed with its human receptor. Proc. Natl. Acad. Sci. U. S. A. **106:**19970–19974.
45. **Yang, B., M. H. Hoe, P. Black, and R. C. Hunt.** 1993. Role of oligosaccharides in the processing and function of human transferrin receptors. Effect of the loss of the three N-glycosyl oligosaccharides individually or together. J. Biol. Chem. **268:**7435–7441.
46. **Zadori, Z., J. Szelei, M.-C. Lacoste, P. Raymond, M. Allaire, I. R. Nabi, and P. Tijssen.** 2001. A viral phospholipase A2 is required for parvovirus infectivity. Dev. Cell **1:**291–302.
47. **Zhou, H., and Y. Zhou.** 2002. Stability scale and atomic solvation parameters extracted from 1023 mutation experiments. Proteins **49:**483–492.